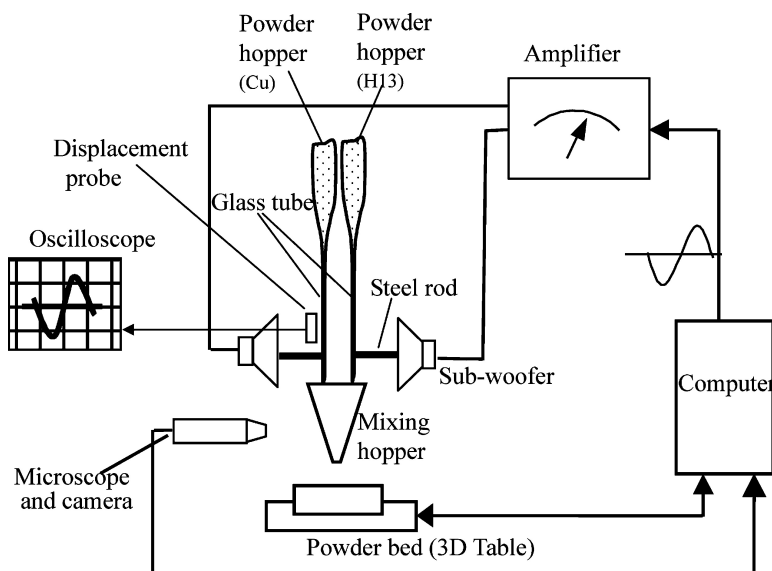


Device for Preparing Combinatorial Libraries in Powder Metallurgy

Shoufeng Yang, and Julian R. G. Evans

J. Comb. Chem., **2004**, 6 (4), 549-555 • DOI: 10.1021/cc040026c • Publication Date (Web): 07 May 2004

Downloaded from <http://pubs.acs.org> on March 20, 2009



More About This Article

Additional resources and features associated with this article are available within the HTML version:

- Supporting Information
- Links to the 1 articles that cite this article, as of the time of this article download
- Access to high resolution figures
- Links to articles and content related to this article
- Copyright permission to reproduce figures and/or text from this article

[View the Full Text HTML](#)

Device for Preparing Combinatorial Libraries in Powder Metallurgy

Shoufeng Yang and Julian R. G. Evans*

Department of Materials, Queen Mary, University of London, Mile End Road, London, E1 4NS U.K.

Received January 13, 2004

This paper describes a powder-metering, -mixing, and -dispensing mechanism that can be used as a method for producing large numbers of samples for metallurgical evaluation or electrical or mechanical testing from multicomponent metal and cermet powder systems. It is designed to make use of the same commercial powders that are used in powder metallurgy and, therefore, to produce samples that are faithful to the microstructure of finished products. The particle assemblies produced by the device could be consolidated by die pressing, isostatic pressing, laser sintering, or direct melting. The powder metering valve provides both on/off and flow rate control of dry powders in open capillaries using acoustic vibration. The valve is simple and involves no relative movement, avoiding seizure with fine powders. An orchestra of such valves can be arranged on a building platform to prepare multicomponent combinatorial libraries. As with many combinatorial devices, identification and evaluation of sources of mixing error as a function of sample size is mandatory. Such an analysis is presented.

Introduction

A combinatorial approach to materials development is slowly gaining acceptability in academic and industrial environments that have traditionally been persuaded by the predictive value of current structure–property relationships.¹ In materials, the demands placed upon combinatorial methods are different from those that prevail in combinatorial chemistry and drug discovery. Importance is often attached to phase volume fraction, particle size of the discontinuous phase, and interfacial interactions rather than just the chemical composition of a single material. These have a commanding effect on physical and mechanical properties in multiphase and composite materials. They are often not predicted well by theory. The need in combinatorial discovery of powder-based materials is, therefore, to provide samples for high-throughput screening which faithfully reproduce the starting materials, such as particle size and distribution, and the processing conditions, such as compaction pressure and sintering profile.

With these ideas in mind, we have built a device for creating multicomponent assemblies of dry powders. This dispensing method has also been applied to solid-freeforming of three-dimensional functional gradients of dry powder for selective laser sintering.² This is a method of creating a complex multifunctional object in which both shape and the three-dimensional spatial arrangement of materials can be downloaded from a computer file concurrently and created layer-by-layer on a building platform. It is important to recognize that any device that can achieve this end for solid-freeforming is, ipso facto, a combinatorial instrument and that some combinatorial instruments are also so-called second-generation solid-freeforming devices.³

The metering and dispensing of dry powders is an essential part of many production processes including, inter alia, the

dosing of pharmaceutical products, ceramic and metal powder compaction, and the blending of paint and printing ink pigments. Most dispensing methods involve mechanical devices.⁴ Examples include helical screw dispensers⁵ and electromagnetically operated plungers.⁶ To avoid the relative movement that can result in seizure and wear and with a quest for simplicity and miniaturization, we selected acoustic control of dispensing in fine capillaries. This method of powder dispensing has its origins in the sand paintings of the Navajo Indians⁷ and has also been proposed as a solid freeforming method for cementitious powders. In it, the flow of powder down the capillary is arrested if vibration stops because domes form in the tube. The rate of flow can be adjusted by changing the amplitude and frequency of acoustic vibration of the tube perpendicular to the flow direction. Thus by sending sound patterns, each generated by computer from a software request for a particular composition, a multitude of samples can be generated on the building platform.

Experiment Details

The powders used to assess the instrument were grade H13 tool steel (0.38% C, 4.9% Cr, 1.7% Mo, 1.0% V, 0.93% Si, 0.32% Mn, balance Fe, 212 μm , from Osprey Metals, Neath, Wales) and oxygen-free high-conductivity copper powder (63–212 μm , from Osprey Metals, Neath, Wales). The particle size distributions of H13 and Cu are shown in Figure 1. The H13 powder was sieved to narrow cuts (delineated in Figure 1) to study the effect of powder size on flow. Binary libraries were prepared from the $\leq 90\text{-}\mu\text{m}$ cut of H13 and 63–212 μm cut of Cu powder in the dual powder delivery experiments.

The powder delivery device consisted of glass capillary tubes of inside diameter 380–600 μm drawn from 10 mm (i.d.) tubes, which acted as the hoppers, and one glass hopper with an orifice of 800 μm , which acted as a mixing hopper, as shown in Figure 2. This diameter range for the glass

* Corresponding author. Phone: +44-20-7882-5501. Fax: +44-20-8981-9804. E-mail: j.r.g.evans@qmul.ac.uk.

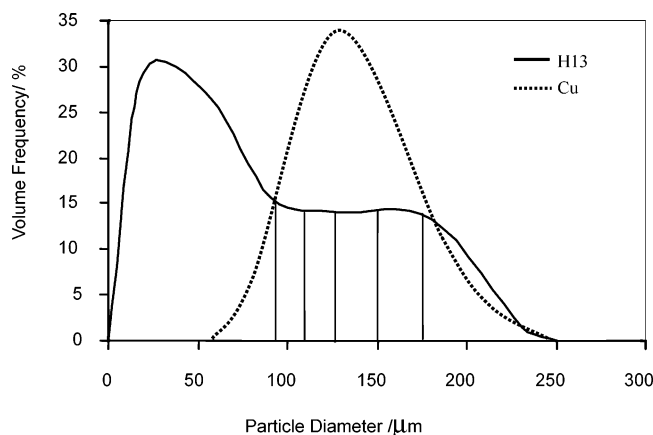


Figure 1. Particle size distribution for gas-atomized H13 tool steel and copper supplied by Osprey Metals (Neath, Wales). The vertical lines represent H13 cuts taken by sieving.

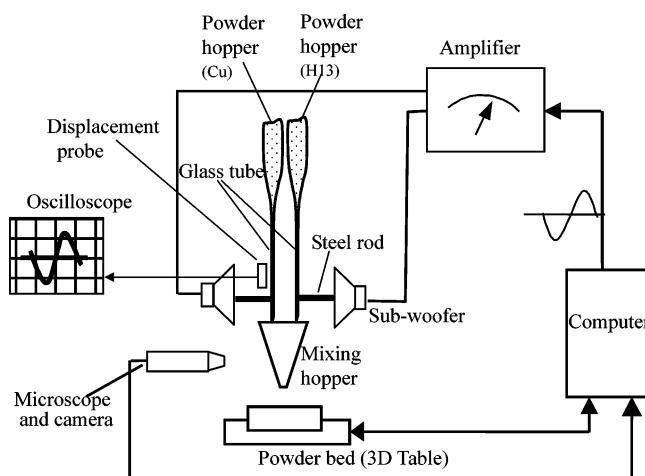


Figure 2. Schematic diagram of the apparatus used for powder flow control and measurement.

capillary tubes gave on/off switching and flow rate control for the test powders used. The orifice diameter of the mixing hopper was selected to balance the formation of a narrow delivery track with the minimum possibility of blockage of powder at the orifice. Acoustic vibration was provided by a

power bass driver (254 mm, 80 W, 40 Hz–4 kHz; from RS Components, Corby, U.K.), the cone center of which was connected to the end of the tube by a 1 mm diameter and 50 mm length steel rod. The vibration was supplied from a 2×30 W amplifier by sound generated using software on a personal computer.

A sensitive noncontact displacement probe (Distec, model 915,250, 1.25 in., from Graham and White Instruments, St. Albans, U.K.) was used to record the true displacement of the tube. This sensor has an output of 7.9 kV m^{-1} . The output of the sensor was monitored by a two-channel 60 MHz digital oscilloscope (Tektronix, TDS210, Tektronix, Inc., U.S.A.) interfaced to the computer. The flow rate of the powder was measured using a four-decimal point balance (TR-104, Denver Instrument Co., USA) interfaced to the PC. The reading of the balance was recorded every second. The tube was illuminated by two high-power LEDs and viewed with a low-power ($\times 10$) optical microscope fitted with a CCD camera. Flow was further viewed and recorded using a high-speed camera, Kodak Ektapro Hs Motion Analyzer, model 4540 (Eastman Kodak Co., San Diego, CA).

Results and Discussion

When no vibration was transmitted to the capillary, the powder stopped flowing because a dome formed in the tube. The ideal capillary radius, R , was thus dependent on the powder characteristics, notably the radius r_p . It is well-known that at $R/r_p > 5$, flow cannot be arrested⁸ and in this work, at $R/r_p < 2$, flow was difficult to initiate.⁹ The value of R is, thus, dependent on each individual powder, but since the capillaries are made by drawing a glass tube and because there is scope to vary R/r_p within limits of $\sim 20\%$ for each powder, it is a simple matter to select an appropriate tube from a collection of drawn capillaries.

The dominant parameters for flow rate control are amplitude and frequency. Figure 3 shows flow rate as a function of reciprocal amplitude for the H13 powder. At infinite amplitude, the curves tend to the origin, because the powder remains arrested on the tube wall by the lateral

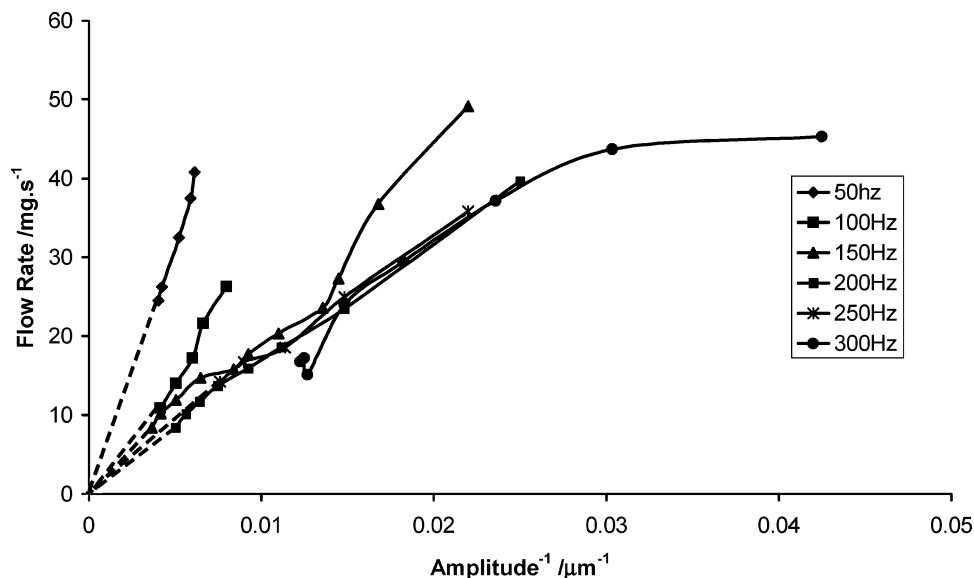


Figure 3. Plot of powder flow rate vs reciprocal amplitude at different frequencies for unseived H13 powder (tube diameter, $450 \mu\text{m}$).

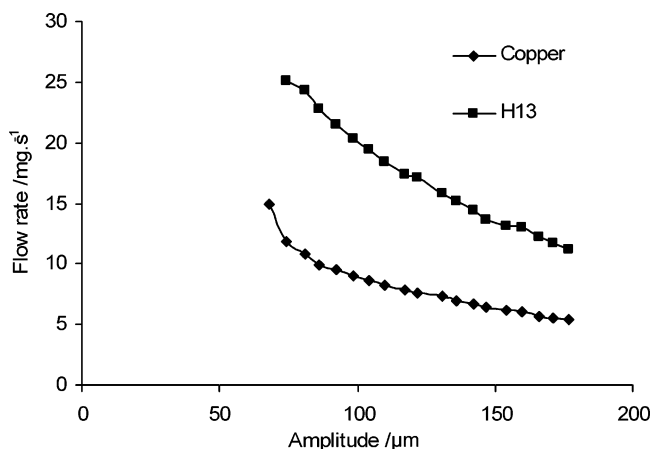


Figure 4. Flow rate of H13 ($\leq 212 \mu\text{m}$ cut) as a function of amplitude at 200 Hz and of Cu ($63\text{--}212 \mu\text{m}$ cut) in tube of inside diameter $450 \mu\text{m}$.

acceleration of the tube. At finite amplitudes, the flow is controlled by the intermittent arrest on the tube walls, the duration of which depends on the fraction of the cycle for which the gravitational force cannot overcome the frictional force. In the remaining part of the cycle, the powder can freefall but must reinitiate its descent twice on each cycle. A fully analytical model has been derived to account for the flow rate control¹⁰ and when plotted confirms the approximate inverse dependence on amplitude.

The value of instruments for combinatorial library construction rests partly on speed of delivery but largely on the mixing errors associated with small samples. The device was, therefore, assessed for the factors that control mixing accuracy. The flow rates of the H13 and copper are indicated by Figure 4 for tubes of $450 \mu\text{m}$ diameter. The effect of waveform on flow rate is marginal, because the generation of square, saw-tooth, or triangular forms result in a similar sine curve when applied to the mechanical system of the valve, as detected by the in situ sensor.²

The combinatorial instrument requires at least two such valves supported over a mixing hopper, each independently vibrated from the computer according to compositional data. Hardware to generate up to eight independent signals is now widely available (e.g., Creative Sound Blaster Audigy 2 NX). The accuracy of mixing depends on (i) the error in flow rate, (ii) the delay at initiation of flow, and (iii) the overflow mass that continues to fall from the tube after vibration stops.

The flow rate was recorded over 500 s at 1 s intervals by a four-decimal point balance. Linear fitting of such mass-time curves always gave a very high correlation coefficient ($R^2 > 0.9999$). Due to continuous impact of powder on the balance pan and the time needed by the balance to adjust, the output at every interval does not reflect the true mass of powder on the balance at that instant. Subtracting two adjacent increments normally gave a maximum difference of 10%, but this does not reflect the error in the absolute mass. An average of readings over 20 s was used to calculate one value of flow rate, and 25 such flow rates were used to calculate the flow rate error. A typical 95% confidence limit (CL) of these 25 flow rate samples was 0.6–0.8% of the mean.

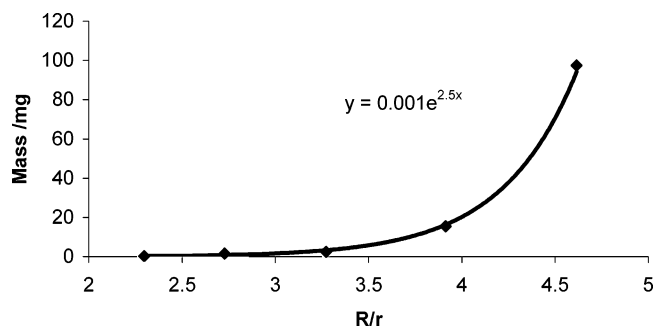


Figure 5. Overflow mass of H13 tool steel powder as a function of R/r_p .

The error due to the delay at initiation of flow was not significant and could be omitted. The initiation of flow was observed by high-speed photography. The particles began to fall within the first half cycle of vibration (at 200 Hz), and the waveform became stable within the first few cycles, the exact number depending on frequency. The maximum error was of the order of a millisecond, corresponding to $25\text{--}50 \mu\text{g}$. If frequencies for each powder are similar, the delays are similar for each powder, so the error tends to be neutralized. However, it is experimentally very difficult to measure the flow rate precisely in the first few cycles. The microscopy of powder tracks deposited at constant velocity of platform travel failed to show a difference at the start of the track, but this is only a qualitative indication of uniformity.

Another error is introduced by the delay caused by the distance between the orifice of the tube and the library platform. Presently, this distance is $\sim 0.1 \text{ m}$ (the length of the mixing hopper), so there will be a 0.14 s delay, but careful engineering could reduce this distance to $\sim 0.01 \text{ m}$ using an optimized spatial arrangement for multiple dispensing valves. This only causes an error when flow rate is changed in a continuous multicomposition delivery because the position of the building platform is different from that position at which the composition was changed. This difference can be predicted exactly and compensated from the computer by changing the composition slightly earlier than required.

The main factor influencing mixing error is the overflow mass, which is strongly dependent on the ratio R/r_p . This mass can be brought down to 1 mg, as shown in Figure 5 provided the lowest possible value of R/r_p is selected. It follows that mixing accuracy can be strongly dependent on sample size, because the overrun is an absolute mass incurred at silence (switching off the acoustic wave). All fluid valves have finite overrun, usually associated with inertial effects. In fact, the value that matters is the error associated with overrun, rather than the mean value of overrun because the latter can be programmed into the software to provide a reduction in delivery interval.

If the overrun mass is 0, the sample mass average and the flow rate (sample mass divided by vibration time) should be independent of sample size or vibration time. Steady-state flow rates (the effective rates at very large flowing time) were acquired from the gradients of 500 s flow records of mass vs time. These flow rates were very stable over this period and gave an error below 0.8%. Sample masses for

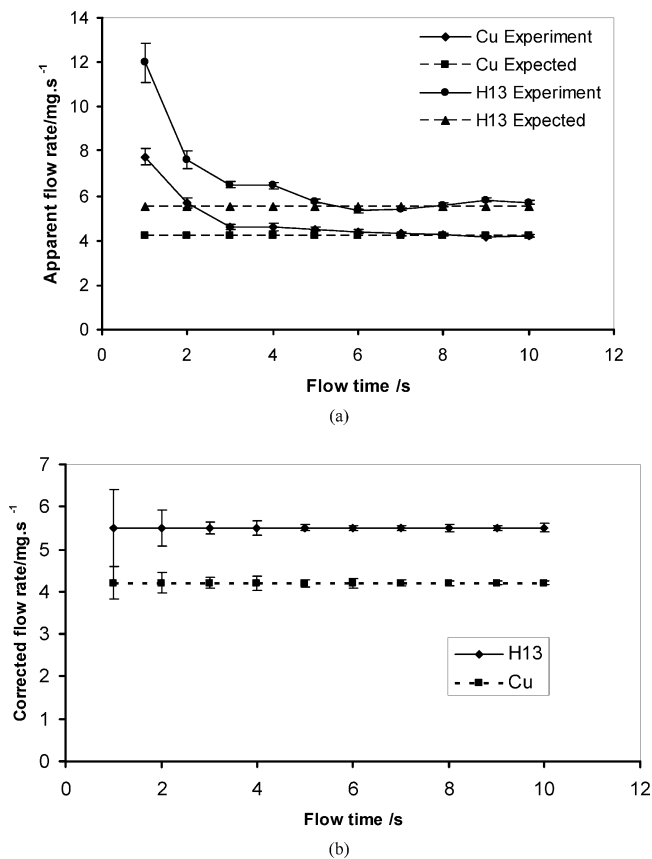


Figure 6. Accuracy of sample size at different flow times of H13 ($\leq 90\text{-}\mu\text{m}$ cut) and copper ($63\text{--}212\ \mu\text{m}$ cut) flow at 200 Hz, $330\ \mu\text{m}$ amplitude in $440\ \mu\text{m}$ tube.

short intervals in multiples of 1 s were then recorded from 1 to 10 s of vibration. The $\leq 90\ \mu\text{m}$ H13 powder and $63\text{--}212\ \mu\text{m}$ copper powder were delivered from a $440\ \mu\text{m}$ i.d. tube by 200 Hz and $330\ \mu\text{m}$ amplitude of vibration. An interval of 10–20 s of silence was inserted between deliveries to leave the powder totally stationary and to let the balance stabilize. Each vibration period was repeated 50 times.

The results are shown in Figure 6a. Under these conditions, the steady-state flow rates of H13 and copper are 5.5 and 4.2 mg/s, respectively. The ordinate gives effective flow rates based on delivery times in multiples of 1 s. The deviation decreased as sample size increased, because the fixed overrun mass was averaged by the sample size. It is close (within 5%) to the expected value when the sample size is greater than ~ 30 mg. In practice, the value of the overrun mass is influenced by particle size, powder composition, tube

diameter, vibration frequency, and amplitude.^{9,11} Part of the calibration procedure is to identify this parameter.

The software can correct for the mean overrun mass, M_{xs} by subtracting it from the specified mass, M , provided $M > M_{\text{xs}}$. In fact, the mean overrun mass itself varies with flow time, t , being 7 and 4 mg at $t = 1$ s and $t = 2$ s, respectively, but 1.5 mg for the average of the subsequent durations, so the overrun mass is a function of mass M , which is $M_{\text{xs}}(M)$. The profile of this function can be acquired from the calibration procedure and stored in the computer as a compensation database. After subtracting this overrun mass, the error in the corrected flow rate was shown in Figure 6b. The errors decreased as sample size increased. The residual error after correction is due to the error in overrun mass itself. Thus, when compensated, the error bars in Figure 6 are displaced to the horizontal curve at 5.5 mg and narrow steadily at increased sample size, thus allowing samples of 16.5 mg to be accurately dispensed.

A wide range of possible sample configurations can be delivered by this device, because the library is assembled on a three-axis table. There are at least four choices for consolidation of the powder. Ideally, the consolidation process should map onto the intended fabrication path for the material. In materials science, properties are causally influenced by processing parameters as well as by composition.

In Figure 7, samples in the copper–H13 binary are dispensed into an alumina library well plate prepared by laminating a perforated alumina tile to an unperforated base. The compositions are at 10 wt % intervals. In this case, the recesses were 4 mm in diameter and 1 mm deep. This configuration is ideal for samples that are to be melted. The sample mass in these well plates is ~ 60 mg. The error depends on composition, being greater at either end of the composition scale.

In a series of fixed masses in a sample library with various compositions, the error, $\text{Err}(W_{\alpha}, M)$, of any component α can be expressed as

$$\text{Err}_{(W_{\alpha}, M)} = \left| \frac{M_{\alpha} - W_{\alpha}}{W_{\alpha}} \right| \times 100\% \quad (1)$$

where M is the whole sample mass, M_{α} is the delivered mass of component α in the sample, and W_{α} is the expected mass fraction of composition α . Due to the existence of overrun

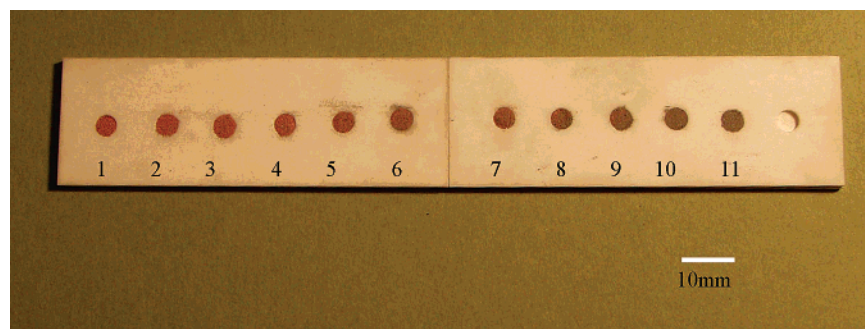


Figure 7. Cu–H13 mixture in ceramic well plate. From left to right: no. 1, 100% Cu; no. 2, 90% Cu–10% H13; no. 3, 80% Cu–0% H13; ...; no. 11, 100% H13.

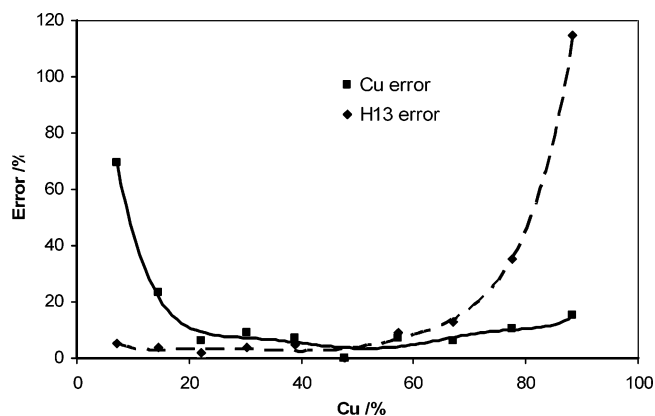


Figure 8. Errors in H13 and Cu contents for a sample size of 60 mg in the ceramic well plate of Figure 7, calculated from the accuracy of sample size in Figure 6.

mass $M_{xs}(M)$, M_{α} can be written as the sum of the expected value and overrun mass.

$$M_{\alpha} = MW_{\alpha} + M_{xs}(M) \quad (2)$$

Substituting eq 2 in eq 1, we get

$$\text{Err}_{(W_{\alpha}, M)} = \frac{M_{xs}(M)}{MW_{\alpha}} \times 100\% \quad (3)$$

From eq 3, we see that the error will increase as sample size M decreases and will increase as composition W_{α} decreases. Because the overrun mass error $M_{xs}(M)$ can be acquired from experiments, the whole error $\text{Err}(W_{\alpha}, M)$ is predictable. The errors in Cu and H13 of 60 mg composite mass were calculated from the accuracy of sample sizes in Figure 6 and are shown in Figure 8. The error of each component decreases as its composition increases. Because the overrun mass of H13 is larger than Cu, the error of H13 at low H13 contents is bigger than that for Cu, which is in agreement with eq 3.

This error can be reduced by avoiding the arrest of flow, thus eliminating error factor iii and accepting only the flow rate errors. This is shown in Figure 9, where elongated slots in extruded and sintered zirconia are used as the well plate.

Well plates in the form of elongated injection molded ceramic boats could also be used, taking care to fill the wells in midrun of the dispensing process. In this way, the powder deposit is only collected when steady flow has been established and composition errors are $<0.8\%$.

The use of elongated strips also lends itself well to selective laser sintering,¹² in which laser power variables can be superimposed on compositional paths orthogonally, as shown in Figure 10, in order to judge how much extra laser power is needed for higher fractions of the more refractory component. This allows a binary composition to be meshed with a sintering variable, such as the laser power needed to eliminate porosity, in a single library.

An alternative and more conventional consolidation path is die or isostatic compaction followed by sintering. This is illustrated in Figure 11, in which a library consisting of copper and H13 tool steel was rendered onto the plunger of a 40 mm diameter steel die. A functional gradient plate was produced in the binary system copper–H13 with H13 powder increasing from 0 to 30 wt % in the z direction. Four layers of copper were delivered, followed by four layers of a mixture of 90% Cu and 10% H13, then four layers of 80% Cu–20% H13, then four layers of 70% Cu–30% H13, then reverting to 100% Cu and repeating this gradient once more. The layer thicknesses were chosen to allow subsequent unambiguous chemical analysis, and the upper limit of H13 was selected to allow sintering to full density. The library was then pressed at 100 MPa and sintered at 1050 °C for 10.8 ks in Ar/4% H₂. The EDX micrograph shown in Figure 11 illustrates the gradient in the direction of increasing tool steel. The melting temperature of H13 is over 1400 °C, so neither copper nor H13 were melted during heat treatment. The sintered sample was cut by a diamond saw lubricated with emulsified cutting oil. In this composite, the hard H13 particles tend to pull out during grinding and polishing, even on the finest grinding paper. So the diamond-cut surface was used for EDX analysis. Only a few small holes were found. The mapping of this surface by EDX (JEOL 6300 equipped with an EDX system, model eXL II, Oxford Instruments, Bucks, U.K.) is shown in Figure 11. The four composition

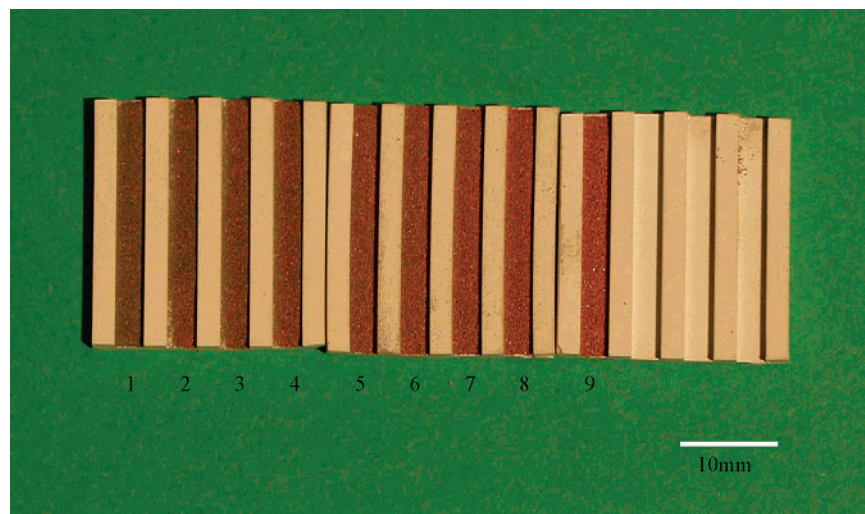


Figure 9. Cu–H13 mixture in slotted ceramic well plate. From left to right: no. 1, 90% Cu–10% Fe; no. 2, 80% Cu–20% Fe; ...; no. 9, 10% Cu–90% Fe.

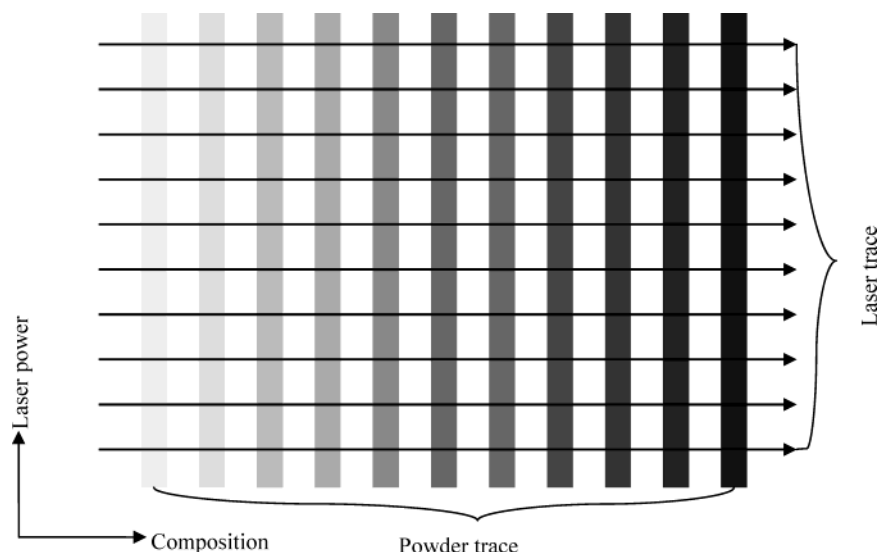


Figure 10. Schematic diagram of a combinatorial search of powder composition/laser power relationships.

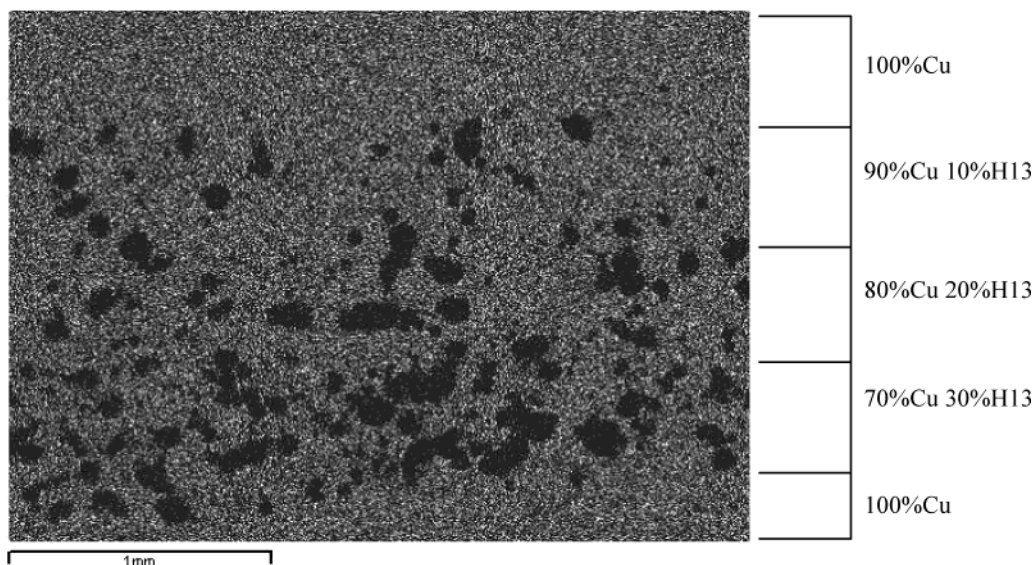


Figure 11. EDX of a sintered powder assembly of a compositional gradient library in the binary copper–tool steel system.

Table 1. Elemental Analysis from EDX for Each Layer in Figure 11

	layers			
	1–4	5–8	9–12	13–16
Cu content expected, wt %	100	90	80	70
Cu content from EDX, wt %	99	90	82	73
H13 content expected, wt %	0	10	20	30
H13 total ^a from EDX, wt %	1	10	18	27

^a Sum of Fe, Cr, V.

zones are defined by the scale in Figure 11, and the compositional analysis results are shown in Table 1. The maximum deviation from the target was 3 wt %. The error associated with quantitative EDX was ~ 1 wt %.

Conclusions

The phenomenon whereby the flow of powder in a capillary can be switched on or off or regulated by acoustic vibration can be used to build a combinatorial powder-dispensing device that is suited to the creation of libraries in powder metallurgy. Various consolidation paths can be applied to the powder assemblies produced in this way. To

demonstrate the device, libraries of copper and tool steel powder were prepared. The sources of errors were discussed, and a method that minimizes the main errors were proposed. The method can use the same commercial powders and the same consolidation procedures as those employed in commercial practice.

Acknowledgment. The authors are grateful to the Engineering and Physical Sciences Research Council for supporting this work under Grant No. GR/N22571.

References and Notes

- (1) Evans J. R. G.; Edirisinghe M. J.; Coveney P. V.; Eames J. *J. Eur. Ceram. Soc.* **2001**, *21*, 2291–2299.
- (2) Yang S.; Evans J. R. G. *Powder Technol.* **2003**, *133*, 251–254.
- (3) Tay B. Y.; Evans J. R. G.; Edirisinghe, M. J. *Int. Mater. Rev.*, in press.
- (4) Coulson J. M.; Richardson J. F. *Chemical Engineering*, 4th ed.; Pergamon Press: Elmsford, NY, 1991; Vol. 2, pp 1–54.
- (5) Johnason, J. R. *Chem. Eng.* **1969**, *76*, 75.
- (6) Yang S.; Evans J. R. G. *Proceedings 2nd Conference of Progress In Rapid Prototyping and Rapid Manufacturing*; Tsinghua University Press: Beijing, 2002; pp 355–359.

- (7) Pegna, J.; Pattofatto, S.; Berge, R.; Bangalan, C.; Herring, H.; LeSaux, M.; Engler, J. *Solid Freeform Fabrication Proceedings*, Austin, Texas, 1997; pp 695–710.
- (8) Kaye B. H. *Powder Mixing*; Chapman and Hall: London, 1997; p 15.
- (9) Yang S.; Evans J. R. G. *Powder Technol.* **2004**, 139, 55–60.
- (10) Yang S.; Evans J. R. G. To be published.
- (11) Yang S.; Evans J. R. G. To be published.
- (12) Bourell D. L.; Marcus H. L.; Barlow J. W.; Beaman J. J. *Int. J. Powder Metall.* **1992**, 28, 369–381.

CC040026C